Published January 23, 2012





**FAK promotes recruitment of talin to nascent adhesions to control cell motility**

Christine Lawson, Ssang-Taek Lim, Sean Uryu, Xiao Lei Chen, David A. Calderwood, and David D. Schlaepfer

Vol. 196 No. 2, January 23, 2012. Pages 223–232.

In the supplemental material originally provided with this paper, incorrect panels appeared in Fig. S3 B. The supplemental PDF has been corrected, and the new panels appear below. The figure legend text also has been revised.

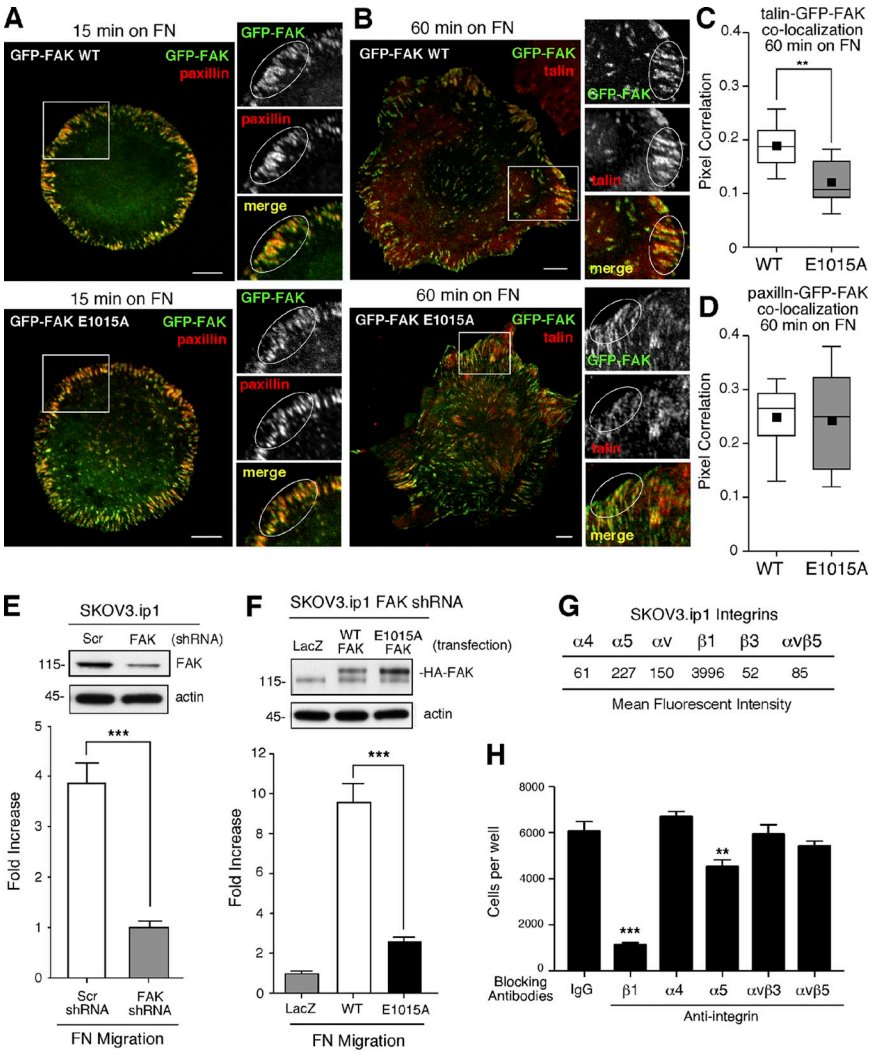


Figure S3. **FAK E1015A localizes to nascent adhesions but does not promote β1 integrin–mediated cell motility.** (A–D) FAK$^{-/-}$ MEFs stably expressing GFP-FAK WT or GFP-FAK E1015A were plated onto FN-coated coverslips for 15 min (A) or 60 min (B), then stained for paxillin (red) and imaged for GFP-FAK (green) fluorescence (A). At 60 min on FN, cells were analyzed for GFP-FAK (green) and talin (red) colocalization (B). The merged image shows colocalization (yellow). Inset, enlarged area of peripheral adhesion staining (circled). Bar, 10 µm. (C and D) The degree of association exhibited by patterns of GFP-FAK and talin (C) or GFP-FAK and paxillin (D) staining was measured on a pixel-by-pixel basis within all adhesions in at least 10 cells per experimental group encompassing at least three independent experiments. Box and whisker plots show the distribution of the data: black square, mean; bottom line, 25th percentile; middle line, median; top line, 75th percentile; whiskers, fifth and 95th percentiles (**, $P < 0.01$). (E) Ovarian SKOV3.ip1 carcinoma cells expressing lentiviral FAK shRNA (or scrambled as control; Scr) were immunoblotted (top) for FAK and actin. (E, bottom) The indicated cells were evaluated for FN-stimulated (10 µg/ml) cell migration (3 h). Data represent the mean ± SEM of three independent experiments (error bars) where FAK shRNA-expressing cell motility was normalized to 1. Significance was determined using an unpaired two-tailed Student's *t* test (***, $P < 0.001$). (F) SKOV3.ip1 FAK shRNA-expressing cells were transiently cotransfected with pCDNA3.1-lacZ and either control vector, HA-tagged FAK-WT, or HA-tagged FAK-E1015A and were immunoblotted (top) for FAK and actin. (F, bottom) The indicated cells were evaluated for FN-stimulated (10 µg/ml) cell migration (3 h). Migratory cells were identified by β-gal staining and counted. Data represent the mean ± SEM of three independent experiments (error bars) where LacZ-transfected cell motility was normalized to 1. Significance was determined using a one-way ANOVA followed by a Tukey multiple comparison test (***, $P < 0.001$). (G) Flow cytometry was used to determine integrin α4, α5, αv, β1, β3, and αvβ5 surface expression, and values represent mean fluorescent intensity using mouse IgG as a control. (H) SKOV3.ip1 cell adhesion to FN-coated (2 µg/ml) dishes was evaluated in the presence of the indicated blocking antibodies to integrins or control IgG. After 15 min, adherent cells were enumerated, and the data represent the mean ± SEM from two independent experiments (error bars). Significance was determined using a one-way ANOVA followed by a Dunnett's multiple comparison test and compared with mouse IgG control group (**, $P < 0.01$; ***, $P < 0.001$).

Published January 23, 2012





# FAK promotes recruitment of talin to nascent adhesions to control cell motility

Christine Lawson,[1] Ssang-Taek Lim,[1] Sean Uryu,[1] Xiao Lei Chen,[1] David A. Calderwood,[2] and David D. Schlaepfer[1]

[1]University of California San Diego, Moores Cancer Center, Department of Reproductive Medicine, La Jolla, CA 92093
[2]Department of Pharmacology, Yale University School of Medicine, New Haven, CT 06520

Cell migration is a dynamic process that involves the continuous formation, maturation, and turnover of matrix–cell adhesion sites. New (nascent) adhesions form at the protruding cell edge in a tension-independent manner and are comprised of integrin receptors, signaling, and cytoskeletal-associated proteins. Integrins recruit focal adhesion kinase (FAK) and the cytoskeletal protein talin to nascent adhesions. Canonical models support a role for talin in mediating FAK localization and activation at adhesions. Here, alternatively, we show that FAK promotes talin recruitment to nascent adhesions occurring independently of talin binding to β1 integrins. The direct binding site for talin on FAK was identified, and a point mutation in FAK (E1015A) prevented talin association and talin localization to nascent adhesions but did not alter integrin-mediated FAK recruitment and activation at adhesions. Moreover, FAK E1015A inhibited cell motility and proteolytic talin cleavage needed for efficient adhesion dynamics. These results support an alternative linkage for FAK–talin interactions within nascent adhesions essential for the control of cell migration.

## Introduction

Integrin-based adhesion assembly and turnover are highly dynamic events underlying cell movement (Parsons et al., 2010). Integrin signals control cell cycle progression, cell survival, and cell polarity, and mediate a linkage to the actin cytoskeleton in the control of cell shape. In spreading cells, edge protrusions are connected to the underlying extracellular matrix via integrin and cytoskeletal structures, termed nascent adhesions, that form concurrently with lamellipodia protrusion (Gardel et al., 2010). Nascent adhesions either disassemble or mature into focal adhesions in part by myosin II–dependent tension generation and actomyosin contractility (Choi et al., 2008). Signaling scaffolding proteins such as FAK, paxillin, RACK1, and talin are rapidly recruited to nascent adhesions (Serrels et al., 2010; Choi et al., 2011). Despite knowledge on protein composition within adhesions, how these sites are formed and remodeled during cell movement remains under investigation.

Talin is a large cytoskeletal protein comprised of an N-terminal head or a band 4.1, ezrin, radixin, moesin homology (FERM) domain that binds to β1 and β3 integrin cytoplasmic tails, type Iγ phosphatidylinositol phosphate (PIP) kinase, and FAK (Calderwood et al., 1999; Di Paolo et al., 2002). The C-terminal talin rod domain binds vinculin and actin, and contains a second integrin-binding site (Critchley and Gingras, 2008). FAK is a cytoplasmic tyrosine kinase that phosphorylates targets such as paxillin in the regulation of adhesion dynamics (Schaller, 2010). FAK is one of the first cytoplasmic proteins recruited to clustered integrins in a tyrosine phosphorylation–independent manner (Miyamoto et al., 1995), and FAK-paxillin binding occurs within nascent adhesions (Choi et al., 2011). Although canonical models also support the importance of talin in the recruitment and activation of FAK at adhesions, FAK connections to talin remain uncharacterized (Chen et al., 1995; Zhang et al., 2008; Frame et al., 2010). As recent three-dimensional nanoscale fluorescent microscopy has co-localized FAK, paxillin, integrin tails, and talin FERM (head domain) to a proximal signaling layer at adhesions followed by the C-terminal part of talin (rod domain) and vinculin localized to a more distal layer (Kanchanawong et al., 2010), we set out to test the importance of FAK–talin binding at nascent adhesions.

Correspondence to David D. Schlaepfer: dschlaepfer@ucsd.edu

Abbreviations used in this paper: ANOVA, analysis of variance; FAT, focal adhesion targeting; FB, fibrinogen; FERM, band 4.1, ezrin, radixin, moesin homology; FN, fibronectin; HUVEC, human umbilical vein endothelial cell; MEF, mouse embryo fibroblast; PIP, phosphatidylinositol phosphate; shRNA, short-hairpin RNA; WT, wild type.



Supplemental Material can be found at:
http://jcb.rupress.org/content/suppl/2012/01/19/jcb.201108078.DC1.html
Original image data can be found at:
http://jcb-dataviewer.rupress.org/jcb/browse/5366

The Rockefeller University Press $30.00
J. Cell Biol. Vol. 196 No. 2 223–232
www.jcb.org/cgi/doi/10.1083/jcb.201108078

Published January 23, 2012

## Results and discussion

### FAK controls talin association with nascent adhesions

FAK knockout ($FAK^{-/-}$) results in an early embryonic lethal phenotype, and $FAK^{-/-}$ mouse embryo fibroblasts (MEFs) form an abundance of adhesions limiting cell movement (Sieg et al., 1999). To study new or "nascent" adhesion formation, $FAK^{-/-}$ and normal ($FAK^{+/+}$) MEFs were trypsinized, held in suspension, and then replated onto fibronectin (FN)-coated glass slides in the absence of serum to synchronize adhesion site formation (Figs. 1 and S1). MEF binding to FN occurs rapidly, and by 15 min, MEFs were spread, and possessed cortical actin rings with low levels of vinculin staining within peripheral paxillin-containing nascent adhesions (Fig. S1 A). Talin strongly colocalized with FAK within nascent $FAK^{+/+}$ MEF adhesions at 15 min (Fig. 1, A and B), and a talin–FAK complex was detected in cell lysates (Fig. 1 C). Strikingly, talin was not localized to nascent $FAK^{-/-}$ MEF adhesions formed at 15 min even though talin expression was equivalent in $FAK^{-/-}$ and $FAK^{+/+}$ MEFs (Fig. 1, A–C). Similar results were obtained upon transient FAK knockdown in human ovarian SKOV3.ip1 carcinoma cells, resulting in the significant reduction of talin–paxillin colocalization within nascent adhesions (Fig. S1, C and D). However, by 60 min on FN, more mature vinculin-containing adhesion sites with integrated actin stress fibers are formed within MEFs (Fig. S1 B) and SKOV3.ip1 cells, and the absence of FAK did not prevent talin localization to these sites (not depicted). Together, these results show that nascent adhesions can form without FAK and that talin recruitment to these sites is enhanced by FAK expression.

### FAK localizes to nascent adhesions independent of talin and adhesion maturation

Previous studies showed that knockdown of talin-1 and talin-2 within MEFs did not prevent initial adhesion formation or spreading on FN, but resulted in reduced integrin activation and mature adhesion formation (Zhang et al., 2008). Interestingly, β1 integrin was localized (not depicted) and activated within nascent adhesions formed at 15 min within $FAK^{-/-}$ and $FAK^{+/+}$ MEFs (Fig. 1 D). Thus, β1 integrin is activated and localized to nascent adhesions without FAK and with limited talin involvement. Talin-1 is the primary isoform expressed in human umbilical vein endothelial cells (HUVECs), and talin-1 knockdown does not alter the kinetics of initial HUVEC spreading at 15 min, but results in reduced cell area and adhesion formation after 1 h (Kopp et al., 2010). Transfection of HUVECs with anti–talin-1 siRNA results in ∼90% knockdown of talin without effects on FAK or paxillin expression (Fig. 1 E). HUVEC spreading on FN at 15 min was equivalent between control- and talin siRNA–expressing cells (Fig. 1 F), and FAK equally colocalized with paxillin at nascent adhesions in talin siRNA–expressing HUVECs (Fig. 1 G). Moreover, the addition of blebbistatin, a pharmacological inhibitor of myosin II that prevents adhesion maturation (Choi et al., 2008), did not prevent FAK colocalization with paxillin or FAK activation upon MEF adhesion to FN (Fig. S2, A and B). FAK transit to nascent adhesions is mediated in part by paxillin binding (Scheswohl et al., 2008), but this is not dependent on talin expression or adhesion maturation.

### Integrin–talin binding is not required for talin recruitment to adhesions

Our results with $FAK^{-/-}$ MEFs and FAK knockdown in SKOV3.ip1 cells support an alternative model whereby FAK facilitates talin recruitment to nascent adhesions. Because talin can bind directly to the cytoplasmic domain of β integrins (Calderwood et al., 1999) and this could link talin to nascent adhesions, FAK–talin recruitment analyses were performed in cells expressing chimeric integrins that support direct talin binding (β1A wild type [WT]) or contain a point mutation in the cytoplasmic domain (β1A Y783A) disrupting talin binding (Fig. 2 A; Nieves et al., 2010). Chimeric integrin-mediated cell adhesion is initiated by plating cells on fibrinogen (FB), and equal numbers of adhesion sites are formed at 15 min in WT and β1A Y783A-expressing cells (unpublished data). At 60 min, β1A Y783A adhesion sites are few in number because of decreased stability (Nieves et al., 2010). Therefore, analyses were performed at 15 min on FB whereby a talin, FAK, and chimeric WT integrin complex was detected by coimmunoprecipitation and was colocalized to nascent adhesions (Fig. 2, B–D). Importantly, in β1A Y783A-expressing cells on FB for 15 min, talin and FAK associate (Fig. 2 B) and are colocalized to adhesions (Fig. 2, C and D) even though β1A Y783A mutation prevents direct talin binding. This result shows that direct talin binding to β1 integrin is not essential for talin recruitment to nascent adhesions.

### Identification of the talin-binding site on FAK

Previous deletion studies identified the FAK C-terminal region (965–1012) and the talin FERM F3 lobe as required for binding (Chen et al., 1995; Borowsky and Hynes, 1998). Pull-down experiments confirmed that FAK 947–1,052 could bind full-length talin independently of paxillin (Fig. 3 A) and that FAK 1,011–1,042 was a minimal region that bound to the talin F2-F3 FERM domain (Fig. 3 B). A direct binding assay using recombinant full-length or C-terminal FAK (853–1,052) and a GST fusion protein of the talin FERM F2-F3 region revealed that FAK–talin interactions were disrupted by talin FERM F3 lobe W359A and A360E mutations (Fig. S2, C and D). As K357A or R358A talin FERM F3 lobe mutations had no effect on FAK–talin interactions (Fig. S2, E and F), these results support FAK binding to talin FERM F3 lobe at a site that may overlap with β integrins (Bouaouina et al., 2008).

Alanine scanning mutagenesis was used to determine residues within FAK 1,011–1,042 required for talin FERM F2-F3 binding (Fig. 3 C). FAK E1015A mutation prevented talin binding. FAK E1015 is a conserved and surface-exposed residue within the FAK focal adhesion targeting (FAT) domain (Fig. 3 D) that does not directly participate in paxillin binding (Hayashi et al., 2002; Gao et al., 2004). In a direct binding assay, in vitro translated full-length WT but not FAK E1015A formed a complex with the GST-talin F2-F3 FERM domain

Published January 23, 2012

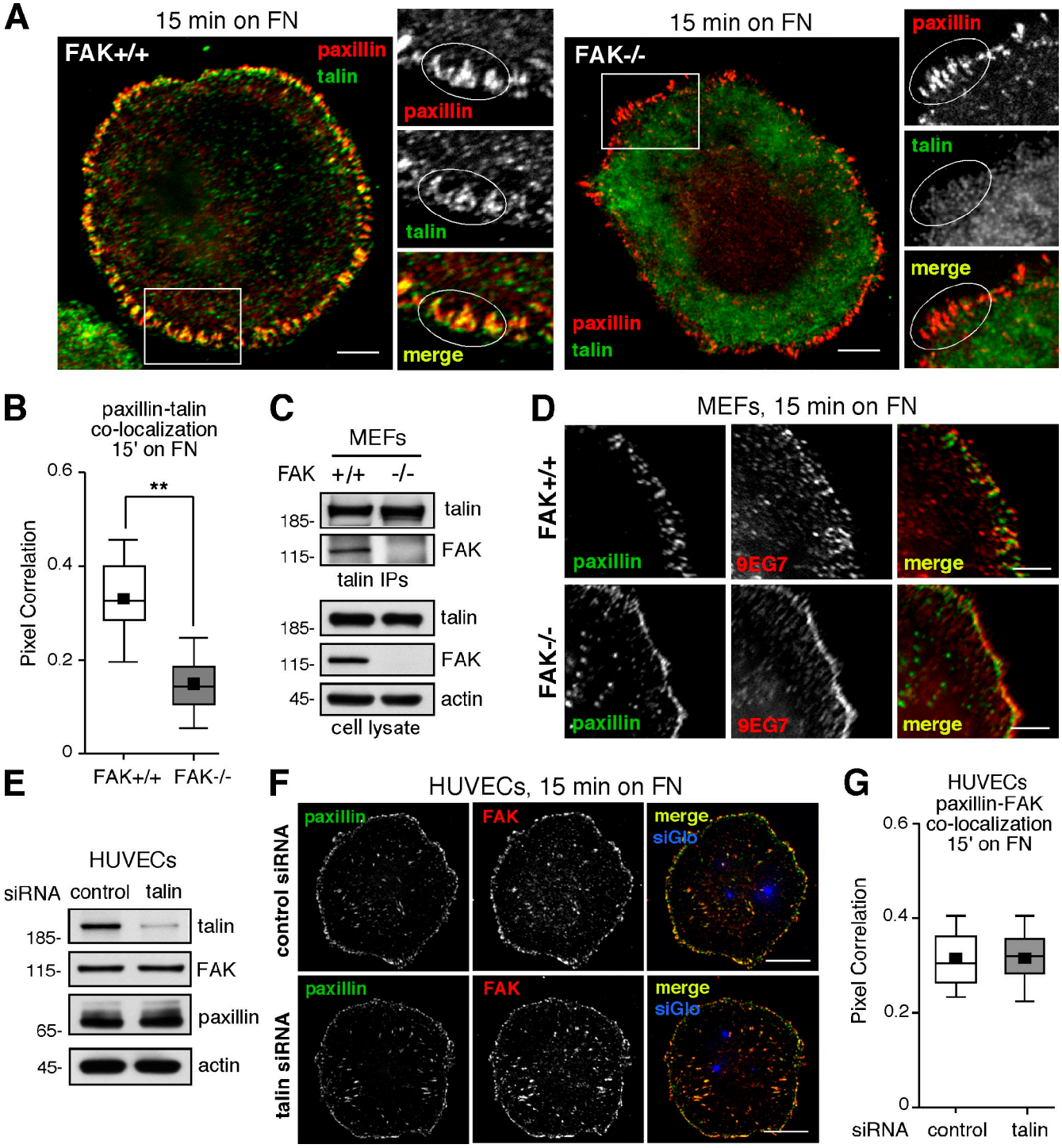


Figure 1. **FAK is required for talin recruitment to nascent adhesions.** (A) FAK$^{+/+}$ and FAK$^{-/-}$ MEFs were serum starved, plated onto FN-coated coverslips for 15 min, and costained with antibodies to talin (green) and paxillin (red). The merged image shows colocalization (yellow). Inset, enlarged area of peripheral adhesion staining (circled). Bars, 10 µm. (B) Cells were analyzed for talin and paxillin colocalization at 15 min on FN (**, $P < 0.01$). (C) Co-immunoprecipitation of FAK with antibodies to talin after cell replating for 15 min on FN. FAK$^{+/+}$ and FAK$^{-/-}$ MEF lysates were analyzed for talin, FAK, and actin expression. (D) Analyses of active β1 integrin (9EG7; red) and paxillin (green) staining of FAK$^{+/+}$ and FAK$^{-/-}$ MEFs plated on FN for 15 min. Bars, 5 µm. (E) Control or anti–talin-1 siRNA transfection of HUVECs and immunoblotting for talin (antibody detects talin-1/-2), FAK, paxillin, and actin expression. Molecular mass is indicated in kilodaltons. (F) Control or anti-talin siRNA transfected HUVECs were replated on FN for 15 min and costained with antibodies to paxillin (green) and FAK (red). Merged image shows colocalization (yellow) and siGlo (blue) transfection marker. Bars, 10 µm. (G) Cells were analyzed for paxillin and FAK colocalization at 15 min on FN. Co-localization was measured on a pixel-by-pixel basis within all adhesions in at least 20 cells per experimental group encompassing at least three independent experiments. Box and whisker plots show the distribution of the data: black square, mean; bottom line, 25th percentile; middle line, median; top line, 75th percentile; whiskers, fifth and 95th percentiles.

Published January 23, 2012

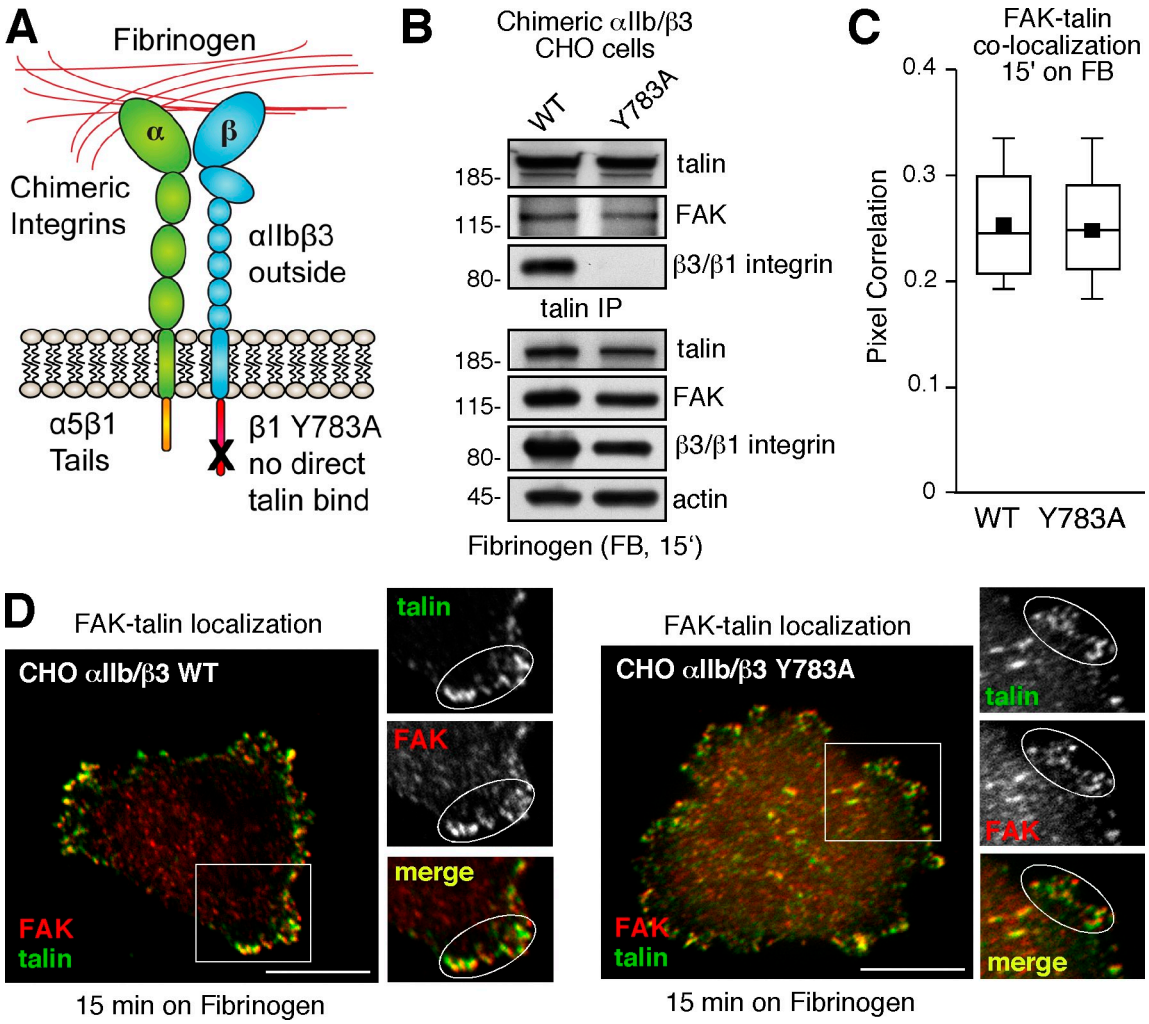


Figure 2. **FAK and talin colocalization at nascent adhesions is independent of direct talin binding to β1 integrin.** (A) Schematic of αIIb-α5/β3-β1 chimeric integrins that bind FB. The β1 cytoplasmic domain is either WT or contains a point mutation (Y783A) disrupting talin binding. (B) Cell lysates were prepared from CHO cells expressing WT or Y783A chimeric integrin plated on FB for 15 min. Talin immunoprecipitates were analyzed by FAK, β3 integrin (to detect chimera), and talin blotting. Lysates were analyzed for talin, FAK, chimeric integrin, and actin expression. Molecular mass is indicated in kilodaltons. (C and D) WT or Y783A chimeric integrin-expressing CHO cells were plated on FB for 15 min and analyzed for endogenous FAK (red) and talin (green) staining. The merged image shows colocalization (yellow). Inset, enlarged area of peripheral adhesion staining (circled). Co-localization analyses and box and whisker plots are described in the legend to Fig. 1. Bars, 10 µm.

(Fig. 3 E). In cells, GFP fusion with FAK WT bound endogenous talin and paxillin, whereas GFP-FAK E1015A bound paxillin but not talin (Fig. 3 F). Together, these results support talin FERM binding to the FAK FAT domain in a manner that is independent of paxillin–FAK binding.

### FAK E1015A prevents talin association within nascent adhesions

FAK$^{-/-}$ MEFs were stably transduced to express GFP, GFP-FAK WT, or GFP-FAK E1015A, and coimmunoprecipitation analyses revealed FAK WT but not FAK E1015A association with talin at 15 min on FN (Fig. 4 A). Both FAK WT and FAK E1015A bound paxillin (Fig. 4 A) and equally colocalized to nascent adhesions at 15 min on FN (Figs. 4 B and S3 A). However, the lack of talin binding to FAK E1015A was also reflected in the significant decrease of talin recruitment to nascent adhesions at 15 min on FN compared with FAK WT reconstituted MEFs (Fig. 4, C and D). At 60 min on FN, there was reduced talin but not paxillin colocalization with GFP-FAK E1015A at adhesions compared with MEFs expressing GFP-FAK WT (Fig. S3, B–D). Partial talin localization to mature adhesions in FAK E1015A MEFs is consistent with alternative localization mechanisms (Franco et al., 2006; Wang et al., 2011). However, as FAK E1015A expression prevents talin recruitment to nascent adhesions, this supports the importance of FAK–talin binding in this process.

### FAK E1015A is activated by FN replating but does not rescue adhesion or motility defects of FAK$^{-/-}$ MEFs

FAK is activated in a cell adhesion–dependent manner as detected by phospho-specific antibodies to the FAK Y397 auto-phosphorylation site upon FN replating (Schaller, 2010). Although FAK WT and E1015A were not phosphorylated under suspended cell conditions, both were rapidly phosphorylated at Y397 within 15 min on FN and remained activated at

Published January 23, 2012

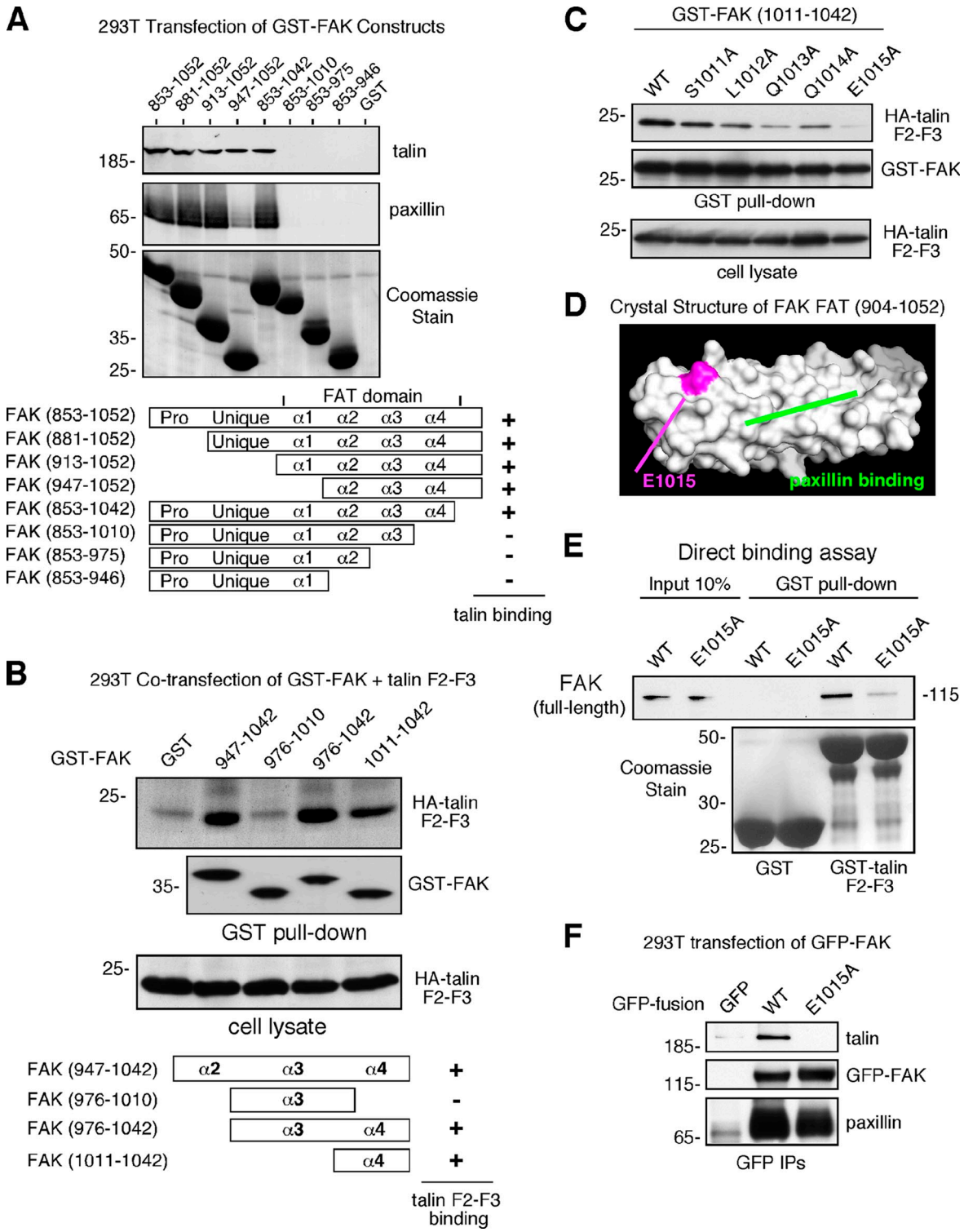


Figure 3. **Talin FERM binds to FAK residues 1,011–1,042 within the FAT domain.** (A) Transient transfection of the indicated GST-FAK C-terminal domain constructs in 293T cells and GST pull-down shows construct size and expression by Coomassie staining. Binding of endogenous paxillin or talin to GST–FAK constructs was determined by immunoblotting. (B) Transient cotransfection of the indicated GST-FAK C-terminal domain constructs in 293T cells and HA-tagged talin FERM F2-F3 was followed by GST pull-down and HA immunoblotting. Equal GST-FAK construct binding to beads and expression of HA-tagged talin FERM was verified by immunoblotting. (C) The indicated alanine point mutations were generated within GST-FAK (1,011–1,042) and cotransfected into 293T cells with HA-talin FERM F2-F3. GST pull-down was followed by HA immunoblotting. Equal GST-FAK construct binding to beads and expression of HA-tagged talin FERM was verified by immunoblotting. (D) Schematic representation of the crystal structure of the FAK FAT domain. E1015 (magenta) is located in the fourth helix of the FAK FAT domain. The paxillin-binding region is indicated (green). (E) In vitro translated full-length FAK WT or FAK E1015A in the presence of biotin-lysine were incubated with GST or GST-talin FERM F2-F3 beads. Direct binding was evaluated by streptavidin immunoblotting with 10% of FAK-WT or FAK-E1015A input as a positive control. (F) 293T cells were transfected with GFP, GFP-FAK-WT, or GFP-FAK-E1015A; replated onto FN-coated dishes for 15 min before lysis; and evaluated for endogenous talin and paxillin association by blotting and anti-GFP immunoprecipitation. Molecular mass is indicated next to the gel blots in kilodaltons.

Published January 23, 2012

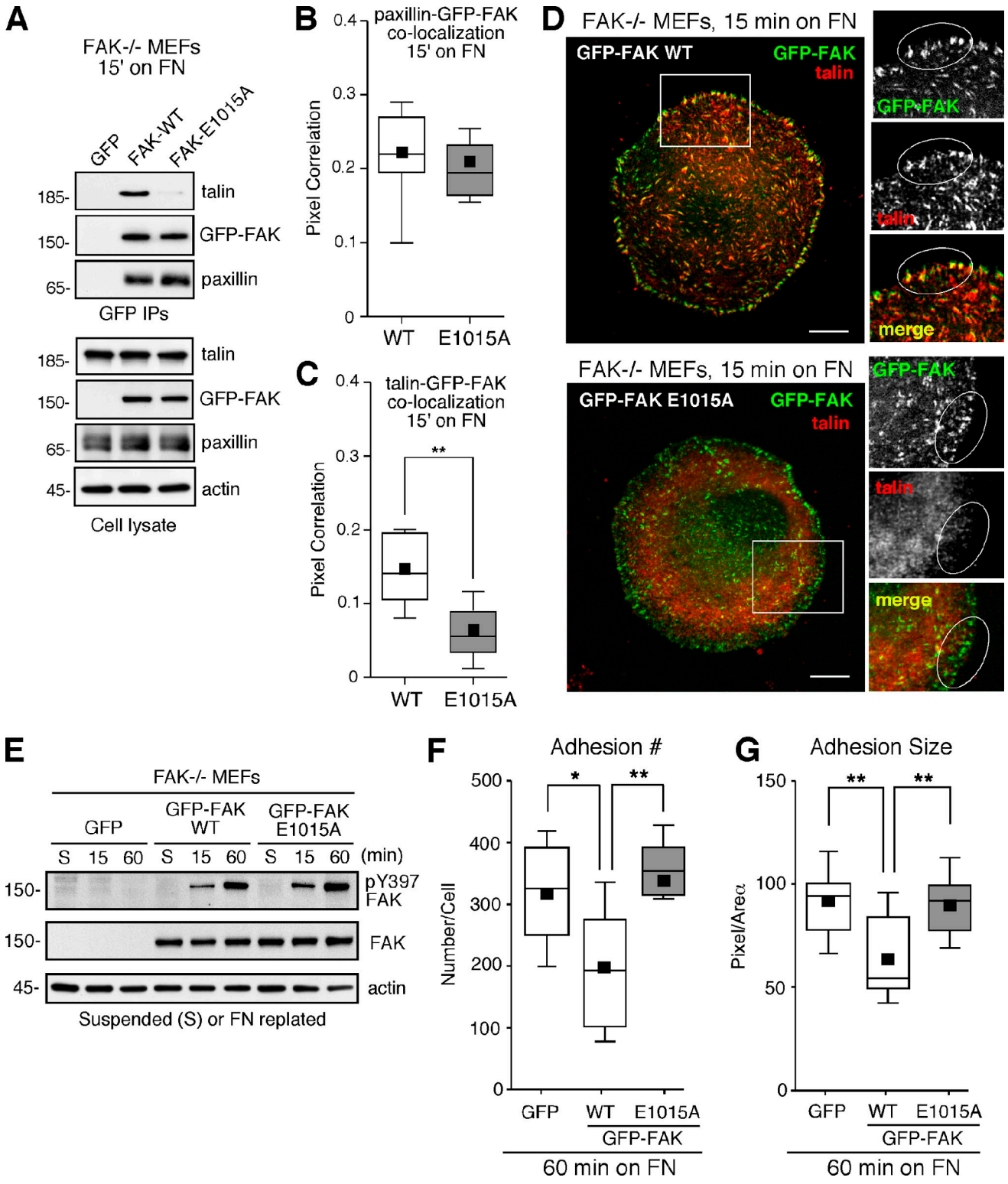


Figure 4. **FAK E1015A expression inhibits talin binding and recruitment to nascent adhesions.** (A) Cell lysates were prepared from FAK$^{-/-}$ MEFs stably re-expressing GFP, GFP-FAK WT, or GFP-FAK E1015A after replating on FN for 15 min. Anti-GFP immunoprecipitates were analyzed for endogenous talin and paxillin association. Lysates were also analyzed for talin, GFP-FAK, paxillin, and actin expression. (B) GFP-FAK WT and GFP-FAK E1015A MEFs were plated on FN for 15 min and analyzed for GPP-FAK (green) and paxillin (red) staining (Fig. S3 A). (C and D) In parallel, cells were analyzed for GPP-FAK (green) and talin (red) staining. Co-localization analyses and box and whisker plots are described in the legend for Fig. 1. Representative images of FN-replated GFP-FAK WT and GFP-FAK E1015A MEFs are shown. The merged images show colocalization (yellow). Inset, enlarged area of peripheral adhesion staining (circled). Bars, 10 µm. (E) FAK$^{-/-}$ MEFs expressing GFP, GFP-FAK WT, or GFP-FAK E1015A were serum starved, suspended (S), and FN replated for the indicated times. Anti-pY397 FAK immunoblotting shows FN-stimulated FAK activation with respect to total FAK and actin levels. Molecular mass is indicated next to the gel blots in kilodaltons. (F and G) Adhesion number (F) and size (G) were determined in the indicated cells at 60 min on FN by anti-paxillin staining in at least 10 cells per experimental group. Box and whisker plots are described in the legend to Fig. 1 (**, $P < 0.01$; *, $P < 0.05$).

Published January 23, 2012

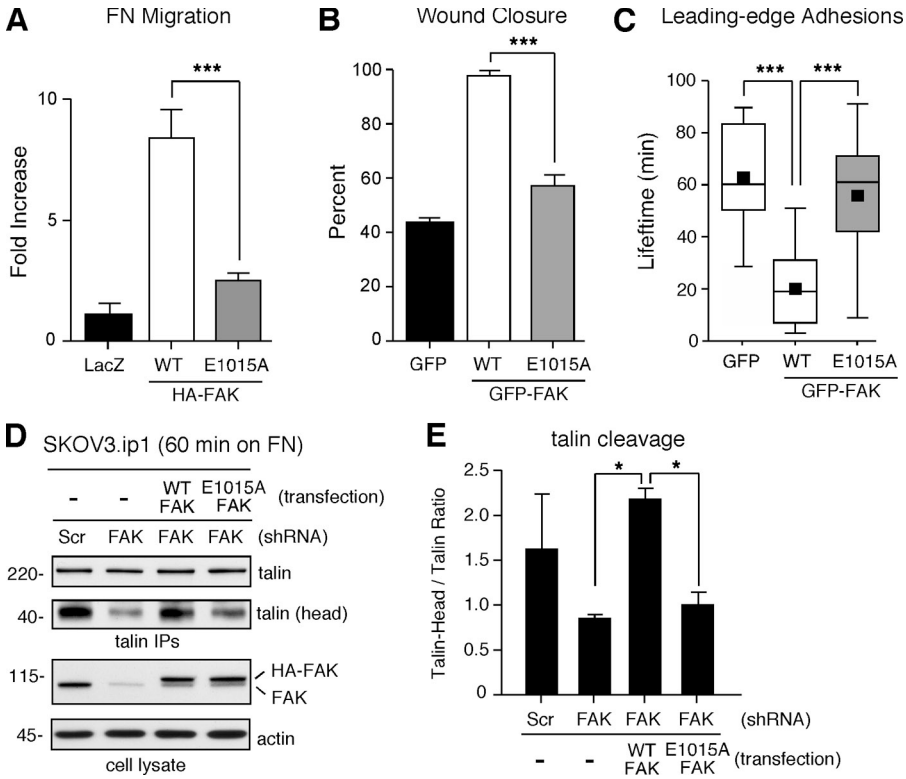


Figure 5. **FAK–talin binding promotes adhesion turnover and cell motility associated with talin cleavage.** (A) FAK$^{-/-}$ MEFs were transfected with the indicated constructs and analyzed for FN haptotaxis cell migration over 3 h. Migratory cells identified by β-gal staining were counted and results normalized to control transfected FAK$^{-/-}$ MEFs. Data are the mean ± SEM of three independent experiments (***, $P < 0.001$). (B) Wound closure motility stimulated by GFP-FAK WT but not GFP-FAK E1015A expression in FAK$^{-/-}$ MEFs. Data are the mean ± SEM of three independent experiments (***, $P < 0.001$). (C) FAK WT but not FAK E1015A reexpression in FAK$^{-/-}$ MEFs decreased leading edge–associated adhesion lifetime. Real-time spinning disk confocal microscopy was used to image mCherry paxillin fluorescence (2 min intervals over 2 h) in wound closure assays. Pixel intensity analyses and adhesion tracking were performed using Image J (version 1.38). Box and whisker plots represent analyses of all newly formed adhesions at the leading edge in at least six cells per experimental group (***, $P < 0.001$). (D) Increased talin cleavage by FAK. Scrambled (Scr) or anti-FAK shRNA SKOV3.ip1 cells were transfected with HA-tagged FAK WT or FAK E1015A and replated onto FN for 60 min. An anti-talin head domain antibody was used for immunoprecipitation, followed by talin, FAK, and actin immunoblotting. Molecular mass is indicated in kilodaltons. (E) Graph showing the ratio of talin head domain to full-length talin by immunoprecipitation and immunoblotting. Data are the mean from two independent experiments (error bars indicate ± SEM; *, $P < 0.05$).

60 min (Fig. 4 E). Thus, talin binding is not essential for integrin-stimulated FAK activation. FAK$^{-/-}$ MEFs exhibit excessive formation of adhesions that accumulate in size and exhibit slow turnover kinetics (Webb et al., 2004). FAK reexpression reverses these defects (Tomar and Schlaepfer, 2009), and adhesion number and size is significantly reduced by GFP-FAK WT compared with GFP-reconstituted FAK$^{-/-}$ MEFs (Fig. 4, F and G). However, GFP-FAK E1015A expression did not reduce adhesion number or size upon FN replating (Fig. 4, F and G). Increased adhesion formation was associated with a threefold reduction of haptotaxis cell motility (Fig. 5 A) and the inhibition of scratch wound closure (Fig. 5 B) by FAK E1015A compared with FAK WT expression. FAK knockdown and reexpression of FAK E1015A in SKOV3.ip1 cells did not promote cell motility initiated by β1 integrin–mediated cell attachment as did FAK WT reexpression (Fig. S3, E–H). Together, these results support the importance of FAK binding to talin in mediating β1 integrin–stimulated cell motility.

### FAK–talin interactions facilitate adhesion dynamics

It is the coordination of adhesion formation and turnover that regulates cell movement, and FAK is intimately involved in these processes (Parsons et al., 2010). Live cell imaging of mCherry-paxillin at wound edge–associated adhesions revealed a mean fluorescence lifetime of 60 min within FAK$^{-/-}$ MEFs, and this was reduced to 20 min upon GFP-FAK WT reexpression (Fig. 5 C). Even though GFP-FAK E1015A was localized to adhesions, these sites exhibited a significantly extended lifetime at wound edges compared with GFP-FAK WT–expressing MEFs (Fig. 5 C). This result is consistent with the inability of FAK E1015A to decrease adhesion number or size. Thus, FAK binding to talin is associated with increased adhesion turnover.

A potential mechanism that may account for increased adhesion lifetime in MEFs lacking FAK or expressing FAK E1015A is that both FAK and talin are substrates of the calpain II protease involved in adhesion turnover (Franco et al., 2004; Chan et al., 2010). Talin cleavage and head domain fragment generation is associated with increased adhesion dynamics (Franco et al., 2004) and elevated integrin activation (Calderwood et al., 1999). Moreover, FAK serves as a scaffold for calpain II recruitment to adhesions (Carragher et al., 2003). To this end, analyses of scrambled short-hairpin RNA (shRNA) or FAK-depleted (FAK shRNA) SKOV3.ip1 cells revealed that FAK knockdown prevented talin head domain fragment generation at 60 min on FN (Fig. 5 D). Re-expression of FAK-WT significantly increased talin head domain generation, whereas FAK-E1015A did not enhance talin cleavage (Fig. 5 E). These results support the importance of a close linkage between talin and FAK in promoting cell motility and adhesion dynamics, in part through enhanced talin cleavage into head and rod domain fragments.

In summary, our results place FAK upstream of talin in mediating nascent adhesion recruitment independent of talin

Published January 23, 2012

binding to β1 integrins. FAK recruitment and activation is associated with integrin clustering, and is independent of talin binding or adhesion maturation. A talin binding mutant of FAK (E1015A) is activated by integrins and is efficiently localized to nascent adhesions, but does not promote adhesion dynamics or cell motility. The presence of a FAK–talin complex within adhesions regulates a cycle of talin proteolysis and focal adhesion turnover enabling cell movement. These studies highlight a new linkage between integrins, FAK, talin, and the control of cell motility.

## Materials and methods

### Cells and constructs

$FAK^{-/-}$ MEFs, $FAK^{+/+}$ MEFs, and human 293T cells were grown and maintained in DME containing 10% FBS, 100 U/ml penicillin, 100 µg/ml streptomycin, MEM nonessential amino acids, and 1 mM sodium pyruvate at 37°C in a 5% $CO_2$ incubator as described previously (Lim et al., 2008). Ovarian SKOV3.ip1 carcinoma cells were from J. Chien (Mayo Clinic, Rochester, MN) and were maintained as described earlier. CHO cells expressing αIIb-5/β3-1A chimeric integrin receptors were from S. LaFlamme (Albany Medical College, Albany, NY) and were cultured in F12 medium with supplements as already described. HUVECs were purchased from Lonza and grown according to the manufacturer's instructions in Endothelial Cell Growth Medium 2 (Lonza) at 37°C in 10% $CO_2$, and cultured on 0.2% gelatin and 10 µg/ml collagen type I coated plastic dishes. HA-tagged talin FERM F2-F3 WT, K357A, R358A, W359A, and A360E constructs were used as described previously (García-Alvarez et al., 2003). mCherry paxillin was from C. Waterman (National Institutes of Health, Bethesda, MD). Primers used in the generation of pEBG FAK mammalian GST fusion proteins, GFP-FAK fusions in pEGFP-C1, GST-talin F2-F3 FERM in pGEX-4T1, or shRNA knockdown constructs in pLentilox 3.7 are detailed in Table S1. Constructs were verified by sequencing.

### Antibodies and reagents

mAb to paxillin (clone M107) was obtained from BD. Rabbit mAb to paxillin (clone Y113) was from Abcam. mAbs to FAK (clone 4.47), to the talin head domain (clone 1676), integrin β1 (clone P4C10), integrin αvβ3 (clone LM609), integrin αvβ5 (clone P1F6), integrin β3 (clone SAP), integrin αv (clone 13C2), integrin α4 (clone HP2/1), and rabbit polyclonal antibodies to FAK (06–543) were from Millipore. Cytochalasin D, latrunculin-A, β-actin (clone AC-17), pan-talin (clone 8d4) mAbs, purified bovine plasma FN, and mitomycin-C were obtained from Sigma-Aldrich. Integrin β3 (clone B-7) mAb was obtained from Santa Cruz Biotechnology, Inc. Rat anti–mouse CD29 (active β1; clone 9EG7) and integrin α5 (clone IIA1) mAbs were from BD. HA-tag (clone 16B12) mAb was from Covance. GST (clone S-tag-05) mAb was from Thermo Fisher Scientific. Phospho-specific rabbit mAb to FAK pY397 (44-625G) was from Invitrogen. Affinity-purified rabbit polyclonal antibodies to FAK 853–1052 were used as described previously (Lim et al., 2008). Integrin α5 (JBS5) antibody was from D. Stupack (University of California, San Diego, La Jolla, CA). Human FB (depleted of von Willebrand Factor and FN) was from Enzyme Research Laboratories. Blebbistatin was from Enzo Life Sciences.

### RNA interference and lentivirus

Human PTK2 (FAK) siGENOME SMART pool siRNA (M-003164-02), siGENOME nontargeting siRNA pool (D-001206-13-05), and siGLO transfection indicator were used (Thermo Fisher Scientific). For siRNA knockdown of human talin1, Stealth Select RNAi (catalog no. 1299003; Invitrogen) oligo 804 (sequence: 5′-CCAAGAACGGAAACCUGCCAGAGUU-3′) was used (Kopp et al., 2010). HUVECs or SKOV3.ip1 cells were transfected with 100 pmol siRNA + 50 pmol siGLO using JetPrime DNA and siRNA transfection reagent (Polyplus Transfection Inc). After 48 h, FAK or talin knockdown was confirmed by immunoblotting. Lentiviral shRNA to human FAK and a scrambled control in pLentiLox 3.7 were created as described previously (Lim et al., 2008) with the primers listed in Table S1. Site-directed mutagenesis of FAK E1015A was performed using QuikChange (Agilent Technologies) and subcloned into pEGFP-C1 FAK as a ClaI–XbaI fragment. GFP and GFP-FAK were subcloned from pEGFP-C1 into the lentiviral vector pCDH1-MCS1-EF1-Puro (System Biosciences) via NheI sites. Lentiviral production was performed as described previously (Lim et al., 2008); target cells were selected with puromycin, sorted by flow cytometry for GFP expression, and maintained as pooled populations.

### Cell replating, protein binding, and immunoblotting

For GST pull-down assays, 293T cells were transfected with plasmids for GST-FAK, HA-talin F2-F3, or empty vector control using JetPrime, and analyzed after 48 h. For replating or imaging experiments, cells were starved (0.5% serum) for 16 h at subconfluent densities, then treated with 0.06% trypsin and 2 mM EDTA in PBS (2.5 min at 37°C). Trypsin was inactivated by the addition of 0.5 mg/ml soybean trypsin inhibitor with 0.25% BSA in DME, collected by centrifugation, resuspended in migration medium (DME with 0.5% BSA), and held at 37°C ($2 \times 10^5$ cells/ml) for 1 h. Acid-washed glass coverslips or plastic culture dishes were coated with FN (10 µg/ml in PBS) or FB (15 µg/ml in PBS) overnight, blocked with 1% BSA in PBS for 30 min, and preheated to 37°C before use in cell experiments. Total protein lysates were prepared after the indicated times in extraction buffer containing 50 mM Hepes, pH 7.4, 150 mM NaCl, 1% Triton X-100, 1% sodium deoxycholate, 0.1% SDS, and 10% glycerol. For immunoprecipitation and GST binding analyses, lysates were diluted twofold in HNTG buffer (50 mM Hepes, pH 7.4, 150 mM NaCl, 0.1% Triton X-100, and 10% glycerol), then incubated with antibodies (1 µg) or glutathione-agarose beads (Sigma-Aldrich) for 3 h at 4°C. Antibodies were collected with either protein A or G Plus (Millipore) agarose beads, and beads washed at 4°C in 1% Triton X-100–only extraction buffer, followed by washes with HNTG buffer, and resolved by SDS-PAGE. For coimmunoprecipitation and binding assays, 5 µM cytochalasin D and 5 µM latrunculin-A were added to cell lysates to disrupt polymerized actin. Immunoblotting was performed with proteins transferred to polyvinylidene difluoride membranes (Millipore) with primary antibodies to FAK (1:1,000), talin (1:25,000), paxillin (1:1,000), GST (1:1,000), HA (1:1,000), actin (1:5,000), β3 (1:200), and pY397 FAK (1:1,000) in Tris-buffered saline containing 2% BSA and 0.05% Tween 20 for 2 h, then visualized by enhanced chemiluminescent detection. Sequential reprobing of membranes was performed as described previously (Lim et al., 2010).

### In vitro translation and direct binding assay

Prey proteins were in vitro translated using the TNT transcription-translation system (Promega). Expression constructs in 1 µg pCDNA3.1 were translated in a mixture containing biotin-labeled lysine and diluted 50-fold into binding buffer (50 mM Hepes, pH 7.4, 150 mM NaCl, and 1% Triton X-100). Bait proteins were expressed as GST fusion proteins in bacteria, prebound to glutathione-agarose beads, incubated with diluted prey protein for 2 h at 4°C, washed three times in binding buffer, resolved by SDS-PAGE, and transferred to PVDF membranes whereby the bait protein was detected by Coomassie staining. The bound prey was detected by streptavidin-horseradish peroxidase immunoblotting. Where indicated, FAK 853–1,052 was expressed as a GST fusion protein, incubated with 50 U/ml thrombin, purified using anion exchange chromatography (Bio-Rad Laboratories), and detected by anti-FAK immunoblotting.

### Cell motility

For transient transfection studies, cells were cotransfected with a pCDNA3-LacZ, HA-tagged FAK-WT, or FAK-E1015A, and evaluated 36 h after transfection. MilliCell chambers (8 µm pores; Millipore) were coated on the membrane underside with 10 µg/ml FN in migration medium for 2 h, washed with PBS, and air dried (30 min) before use. Starved cells (0.5% serum, overnight) were suspended by limited trypsin-EDTA treatment. Soybean trypsin inhibitor (0.25 mg/ml in DME) was added, and cells were pelleted and washed in migration medium (DME with 0.5% BSA) and enumerated (ViCell XR; Beckman Coulter). Cells were held in suspension for 1 h, $10^5$ cells in 0.3 ml were added to each MilliCell chamber, units were placed into 24-well plates containing 0.4 ml migration medium, and cells were incubated for 3 h at 37°C. Cells per microscopic field were counted (nine fields per chamber), and transiently transfected cells were selectively enumerated by staining for β-galactosidase activity using X-gal as a substrate. Mean values were obtained from three individual chambers for each experimental point per assay.

### Immunofluorescent staining

Cells replated for the indicated time on FN or FB glass coverslips (as described earlier) were fixed in 3.7% paraformaldehyde (15 min), permeabilized with 0.1% Triton X-100 in PBS (10 min), and incubated in blocking buffer (2% BSA in PBS) for 1 h. Talin (1:500), paxillin (1:250), activated β1 (9EG7; 1:50), or FAK (1:50) antibodies were diluted in blocking buffer and incubated overnight at 4°C. Coverslips were washed in PBS,

Published January 23, 2012

incubated with Alexa Fluor 488 goat anti–mouse and Alexa Fluor 594 goat anti–rabbit or Alexa Fluor 647 goat anti–rabbit (Invitrogen) diluted in blocking buffer (45 min). Images were acquired sequentially using a mercury lamp source, multiband dichroic, single-band exciter, and single-band emitter filter sets (Chroma Technology Corp.) on dual filter wheels. A spinning disc confocal microscope (IX81; Olympus) at 60× (Plan-Apochromat, NA 1.42 objective lens) and a camera (OrcaER; Hamamatsu) controlled by Slidebook (v5.0) software were used. Files were cropped, pseudo-colored, and contrast-adjusted using Photoshop (Adobe). The degree of association exhibited by patterns of fluorescence was measured on a pixel-by-pixel basis and calculated as a Pearson's correlation coefficient using the "measure correlations" module (Cell Profiler, v2.0; Broad Institute). A value of 0 indicates no overlap and a value of 1 corresponds to 100% colocalization. Adhesion size (pixels) and the number within a cell were determined using Cell Profiler using a pipeline to threshold images and reduce background fluorescent staining.

### Flow cytometry

Cells were trypsinized, enumerated, and incubated with primary antibodies to integrins ($10^6$ cells/µg antibody) for 20 min on ice in 100 µl of PBS, followed by pelleting and washing using cold PBS. Allophycocyanin (APC)-conjugated goat anti–mouse IgG (BD) was used as a secondary antibody, and analyses were performed using a FACS Calibur (BD) with FlowJo software. Mouse IgG was used as a negative control.

### Cell adhesion

Serum-starved cells were trypsinized, enumerated, and held in suspension in migration medium at 37°C for 10 min in the presence of 10 µg/ml of control mouse IgGs or antibodies specific to integrins β1, αvβ3, αvβ5, α4, and α5. Cells (in the presence of antibodies) were evaluated for adhesion to FN-coated (2 µg/ml) dishes at 15 min by paraformaldehyde fixation, crystal violet staining, and counting.

### Scratch-wound, time-lapse imaging, and quantification of FA dynamics

Glass-bottom dishes (MatTek) were coated with 2 µg/ml FN, and cells were plated at a subconfluent density (75%). After 24 h, cells were serum starved overnight, wounded with a pipette tip, washed with PBS, and incubated in growth media containing 0.5 µg/ml of mitomycin-C before imaging. For time-lapse wound healing experiments, images of cells in phase were acquired every 15 min in a humidified 5% $CO_2$ environment at 37°C using a microscope (IX51; Olympus), xy-controlled stage with a z focus drive (Olympus), 10× objective lens (UPLFL, 0.30 NA), a MAC5000 controller and LEP shutter (Ludl Electronics), and a camera (OrcaER; Hamamatsu Photonics) controlled by Slidebook (v5.0) software. Wound closure percentage was calculated by the change in area between 0 and 8 h. For confocal time-lapse microscopy of cells at the leading wound edge, GFP, GFP-FAK-WT, or GFP-FAK-E1015A reconstituted $FAK^{-/-}$ MEFs were transfected with mCherry paxillin as an adhesion marker. Sequential GFP and mCherry images were acquired every 2 min for 2 h in a humidified 5% $CO_2$ environment at 37°C using a control spinning disk confocal microscope with zero drift compensation focus (IX81; Olympus) at 60× (Plan-Apochromat, NA 1.42 objective lens), as well as a mercury lamp source, multiband dichroic, single-band exciter, and single band emitter filter sets (Chroma Technology Corp.) on dual filter wheels, and a camera (OrcaER) controlled by Slidebook (v5.0) software. Files were cropped, pseudo-colored, and contrast-adjusted using Photoshop. Quantification of adhesion dynamics at the leading edge was performed by background subtraction and pixel intensity analyses using ImageJ (version 1.38) software. Adhesion lifetime was determined by thresholding images to select for individual adhesions followed by tracking using an ImageJ (manual tracking) plug-in module.

### Statistical analysis

A two-tailed unpaired Student's *t* test was used to evaluate two groups. Significance between multiple groups was determined by one-way analysis of variance (ANOVA) followed by either Dunnett's or Tukey's multiple comparison test.

### Online supplemental material

Fig. S1 shows nascent and mature adhesion formation upon FN replating and the role of FAK in promoting talin recruitment to nascent adhesions in human ovarian carcinoma cells. Fig. S2 shows that nascent adhesion localization and activation of FAK occurs in a tension-independent manner, and shows experiments with direct talin FERM binding to FAK. Fig. S3 shows that FAK-E1015A localizes to nascent adhesions but does not promote β1 integrin–mediated cell motility. Table S1 summarizes the primers used for PCR cloning, PCR mutagenesis, FAK shRNA, and recombinant FAK protein production. Online supplemental material is available at http://www.jcb.org/cgi/content/full/jcb.201108078/DC1.

We thank Susan LaFlamme (Albany Medical College, NY) for providing chimeric integrin-expressing CHO cells. C. Lawson was supported by a Canadian Institutes of Health Research fellowship, 200810MFE-193594-139144.

This work was supported by National Institutes of Health grants to D. Calderwood (GM068600 and GM088240) and to D. Schlaepfer (GM087400 and CA102310).

The authors declare that they have no competing financial interests.

Submitted: 12 August 2011
Accepted: 12 December 2011

## References

Borowsky, M.L., and R.O. Hynes. 1998. Layilin, a novel talin-binding transmembrane protein homologous with C-type lectins, is localized in membrane ruffles. *J. Cell Biol.* 143:429–442. http://dx.doi.org/10.1083/jcb.143.2.429

Bouaouina, M., Y. Lad, and D.A. Calderwood. 2008. The N-terminal domains of talin cooperate with the phosphotyrosine binding-like domain to activate beta1 and beta3 integrins. *J. Biol. Chem.* 283:6118–6125. http://dx.doi.org/10.1074/jbc.M709527200

Calderwood, D.A., R. Zent, R. Grant, D.J. Rees, R.O. Hynes, and M.H. Ginsberg. 1999. The Talin head domain binds to integrin beta subunit cytoplasmic tails and regulates integrin activation. *J. Biol. Chem.* 274:28071–28074. http://dx.doi.org/10.1074/jbc.274.40.28071

Carragher, N.O., M.A. Westhoff, V.J. Fincham, M.D. Schaller, and M.C. Frame. 2003. A novel role for FAK as a protease-targeting adaptor protein: regulation by p42 ERK and Src. *Curr. Biol.* 13:1442–1450. http://dx.doi.org/10.1016/S0960-9822(03)00544-X

Chan, K.T., D.A. Bennin, and A. Huttenlocher. 2010. Regulation of adhesion dynamics by calpain-mediated proteolysis of focal adhesion kinase (FAK). *J. Biol. Chem.* 285:11418–11426. http://dx.doi.org/10.1074/jbc.M109.090746

Chen, H.C., P.A. Appeddu, J.T. Parsons, J.D. Hildebrand, M.D. Schaller, and J.L. Guan. 1995. Interaction of focal adhesion kinase with cytoskeletal protein talin. *J. Biol. Chem.* 270:16995–16999. http://dx.doi.org/10.1074/jbc.270.28.16995

Choi, C.K., M. Vicente-Manzanares, J. Zareno, L.A. Whitmore, A. Mogilner, and A.R. Horwitz. 2008. Actin and alpha-actinin orchestrate the assembly and maturation of nascent adhesions in a myosin II motor-independent manner. *Nat. Cell Biol.* 10:1039–1050. http://dx.doi.org/10.1038/ncb1763

Choi, C.K., J. Zareno, M.A. Digman, E. Gratton, and A.R. Horwitz. 2011. Cross-correlated fluctuation analysis reveals phosphorylation-regulated paxillin-FAK complexes in nascent adhesions. *Biophys. J.* 100:583–592. http://dx.doi.org/10.1016/j.bpj.2010.12.3719

Critchley, D.R., and A.R. Gingras. 2008. Talin at a glance. *J. Cell Sci.* 121:1345–1347. http://dx.doi.org/10.1242/jcs.018085

Di Paolo, G., L. Pellegrini, K. Letinic, G. Cestra, R. Zoncu, S. Voronov, S. Chang, J. Guo, M.R. Wenk, and P. De Camilli. 2002. Recruitment and regulation of phosphatidylinositol phosphate kinase type 1 gamma by the FERM domain of talin. *Nature*. 420:85–89. http://dx.doi.org/10.1038/nature01147

Frame, M.C., H. Patel, B. Serrels, D. Lietha, and M.J. Eck. 2010. The FERM domain: organizing the structure and function of FAK. *Nat. Rev. Mol. Cell Biol.* 11:802–814. http://dx.doi.org/10.1038/nrm2996

Franco, S.J., M.A. Rodgers, B.J. Perrin, J. Han, D.A. Bennin, D.R. Critchley, and A. Huttenlocher. 2004. Calpain-mediated proteolysis of talin regulates adhesion dynamics. *Nat. Cell Biol.* 6:977–983. http://dx.doi.org/10.1038/ncb1175

Franco, S.J., M.A. Senetar, W.T. Simonson, A. Huttenlocher, and R.O. McCann. 2006. The conserved C-terminal I/LWEQ module targets Talin1 to focal adhesions. *Cell Motil. Cytoskeleton*. 63:563–581. http://dx.doi.org/10.1002/cm.20145

Gao, G., K.C. Prutzman, M.L. King, D.M. Scheswohl, E.F. DeRose, R.E. London, M.D. Schaller, and S.L. Campbell. 2004. NMR solution structure of the focal adhesion targeting domain of focal adhesion kinase in complex with a paxillin LD peptide: evidence for a two-site binding model. *J. Biol. Chem.* 279:8441–8451. http://dx.doi.org/10.1074/jbc.M309808200

García-Alvarez, B., J.M. de Pereda, D.A. Calderwood, T.S. Ulmer, D. Critchley, I.D. Campbell, M.H. Ginsberg, and R.C. Liddington. 2003. Structural determinants of integrin recognition by talin. *Mol. Cell*. 11:49–58. http://dx.doi.org/10.1016/S1097-2765(02)00823-7

Gardel, M.L., I.C. Schneider, Y. Aratyn-Schaus, and C.M. Waterman. 2010. Mechanical integration of actin and adhesion dynamics in cell migration. *Annu. Rev. Cell Dev. Biol.* 26:315–333. http://dx.doi.org/10.1146/annurev.cellbio.011209.122036

Hayashi, I., K. Vuori, and R.C. Liddington. 2002. The focal adhesion targeting (FAT) region of focal adhesion kinase is a four-helix bundle that binds paxillin. *Nat. Struct. Biol.* 9:101–106. http://dx.doi.org/10.1038/nsb755

Kanchanawong, P., G. Shtengel, A.M. Pasapera, E.B. Ramko, M.W. Davidson, H.F. Hess, and C.M. Waterman. 2010. Nanoscale architecture of integrin-based cell adhesions. *Nature*. 468:580–584. http://dx.doi.org/10.1038/nature09621

Kopp, P.M., N. Bate, T.M. Hansen, N.P. Brindle, U. Praekelt, E. Debrand, S. Coleman, D. Mazzeo, B.T. Goult, A.R. Gingras, et al. 2010. Studies on the morphology and spreading of human endothelial cells define key inter- and intramolecular interactions for talin1. *Eur. J. Cell Biol.* 89:661–673. http://dx.doi.org/10.1016/j.ejcb.2010.05.003

Lim, S.T., X.L. Chen, Y. Lim, D.A. Hanson, T.T. Vo, K. Howerton, N. Larocque, S.J. Fisher, D.D. Schlaepfer, and D. Ilic. 2008. Nuclear FAK promotes cell proliferation and survival through FERM-enhanced p53 degradation. *Mol. Cell*. 29:9–22. http://dx.doi.org/10.1016/j.molcel.2007.11.031

Lim, S.T., X.L. Chen, A. Tomar, N.L. Miller, J. Yoo, and D.D. Schlaepfer. 2010. Knock-in mutation reveals an essential role for focal adhesion kinase activity in blood vessel morphogenesis and cell motility-polarity but not cell proliferation. *J. Biol. Chem.* 285:21526–21536. http://dx.doi.org/10.1074/jbc.M110.129999

Miyamoto, S., H. Teramoto, O.A. Coso, J.S. Gutkind, P.D. Burbelo, S.K. Akiyama, and K.M. Yamada. 1995. Integrin function: molecular hierarchies of cytoskeletal and signaling molecules. *J. Cell Biol.* 131:791–805. http://dx.doi.org/10.1083/jcb.131.3.791

Nieves, B., C.W. Jones, R. Ward, Y. Ohta, C.G. Reverte, and S.E. LaFlamme. 2010. The NPIY motif in the integrin beta1 tail dictates the requirement for talin-1 in outside-in signaling. *J. Cell Sci.* 123:1216–1226. http://dx.doi.org/10.1242/jcs.056549

Parsons, J.T., A.R. Horwitz, and M.A. Schwartz. 2010. Cell adhesion: integrating cytoskeletal dynamics and cellular tension. *Nat. Rev. Mol. Cell Biol.* 11:633–643. http://dx.doi.org/10.1038/nrm2957

Schaller, M.D. 2010. Cellular functions of FAK kinases: insight into molecular mechanisms and novel functions. *J. Cell Sci.* 123:1007–1013. http://dx.doi.org/10.1242/jcs.045112

Scheswohl, D.M., J.R. Harrell, Z. Rajfur, G. Gao, S.L. Campbell, and M.D. Schaller. 2008. Multiple paxillin binding sites regulate FAK function. *J. Mol. Signal.* 3:1. http://dx.doi.org/10.1186/1750-2187-3-1

Serrels, B., E. Sandilands, A. Serrels, G. Baillie, M.D. Houslay, V.G. Brunton, M. Canel, L.M. Machesky, K.I. Anderson, and M.C. Frame. 2010. A complex between FAK, RACK1, and PDE4D5 controls spreading initiation and cancer cell polarity. *Curr. Biol.* 20:1086–1092. http://dx.doi.org/10.1016/j.cub.2010.04.042

Sieg, D.J., C.R. Hauck, and D.D. Schlaepfer. 1999. Required role of focal adhesion kinase (FAK) for integrin-stimulated cell migration. *J. Cell Sci.* 112:2677–2691.

Tomar, A., and D.D. Schlaepfer. 2009. Focal adhesion kinase: switching between GAPs and GEFs in the regulation of cell motility. *Curr. Opin. Cell Biol.* 21:676–683. http://dx.doi.org/10.1016/j.ceb.2009.05.006

Wang, P., C. Ballestrem, and C.H. Streuli. 2011. The C terminus of talin links integrins to cell cycle progression. *J. Cell Biol.* 195:499–513. http://dx.doi.org/10.1083/jcb.201104128

Webb, D.J., K. Donais, L.A. Whitmore, S.M. Thomas, C.E. Turner, J.T. Parsons, and A.F. Horwitz. 2004. FAK-Src signalling through paxillin, ERK and MLCK regulates adhesion disassembly. *Nat. Cell Biol.* 6:154–161. http://dx.doi.org/10.1038/ncb1094

Zhang, X., G. Jiang, Y. Cai, S.J. Monkley, D.R. Critchley, and M.P. Sheetz. 2008. Talin depletion reveals independence of initial cell spreading from integrin activation and traction. *Nat. Cell Biol.* 10:1062–1068. http://dx.doi.org/10.1038/ncb1765

Published January 23, 2012



Lawson et al., http://www.jcb.org/cgi/content/full/jcb.201108078/DC1

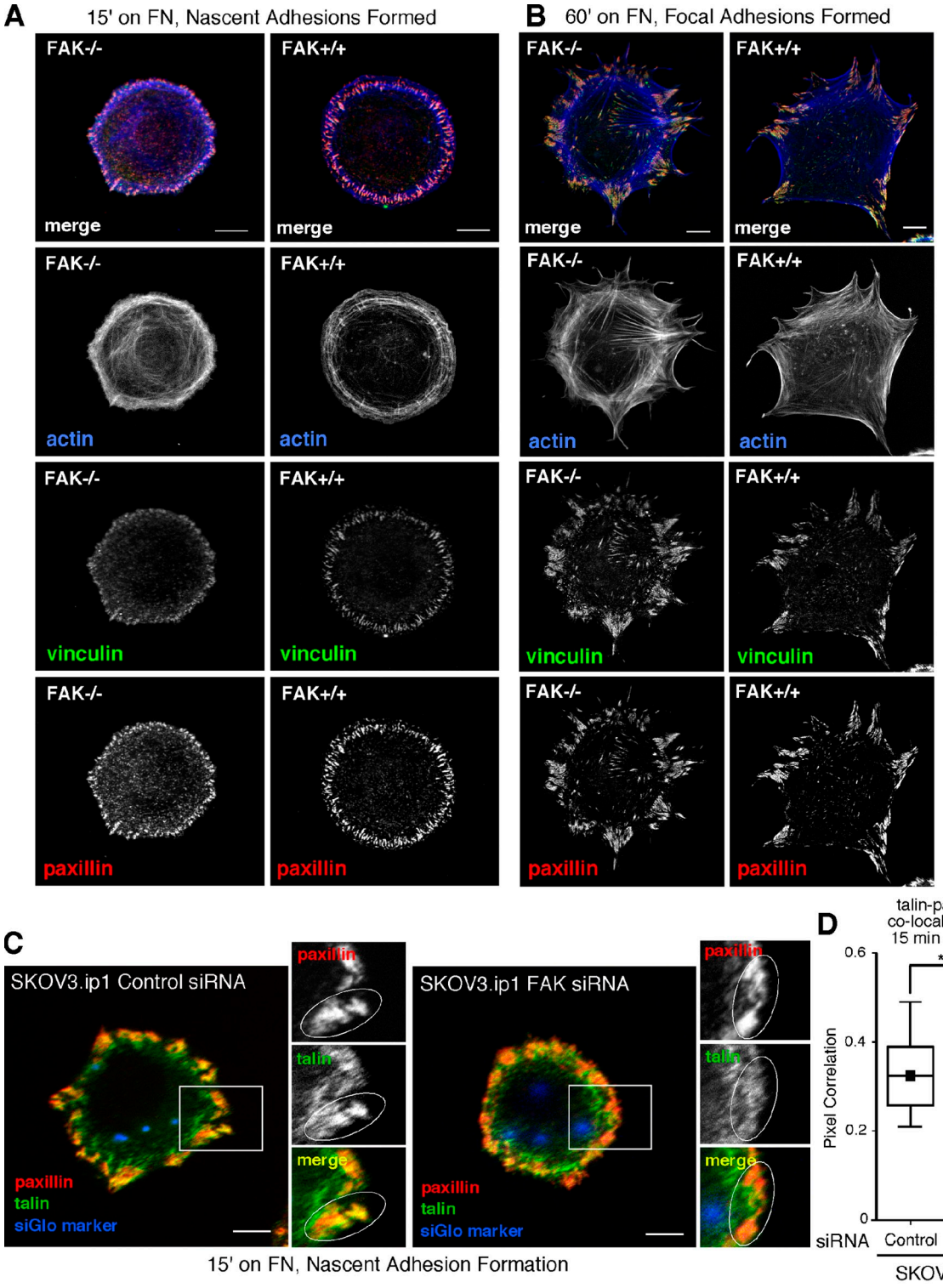


Figure S1. **Time course of adhesion formation upon FN replating.** FAK facilitates talin recruitment to nascent ovarian carcinoma adhesions. FAK$^{-/-}$ or FAK$^{+/+}$ fibroblasts were held in suspension, then replated onto FN-coated (10 µg/ml) glass coverslips in the absence of serum for 15 min (A) for nascent adhesion or 60 min (B) for mature adhesion analyses. Cells were costained to visualize paxillin (red), vinculin (green), and actin (Alexa Fluor 350 phalloidin; blue). Merged images show colocalization (yellow/white). Bar, 5 µm. (C) SKOV3.ip1 ovarian carcinoma cells were cotransfected with anti-FAK siRNA or control siRNA and a transfection indicator (siGlo). Cells were serum starved and plated onto FN-coated coverslips for 15 min. Cells were then costained with paxillin (red) and talin (green), and imaged for siGlo (blue). The merged image shows colocalization (yellow). Inset, enlarged area of peripheral adhesion staining (circled). Bar, 10 µm. (D) Cells were analyzed for talin and paxillin colocalization at 15 min on FN (**, $P < 0.01$). Colocalization was measured on a pixel-by-pixel basis within all adhesions in at least 10 cells per experimental group encompassing at least three independent experiments. Box and whisker plots show the distribution of the data: black square, mean; bottom line, 25th percentile; middle line, median; top line, 75th percentile; whiskers, fifth and 95th percentiles.

Published January 23, 2012

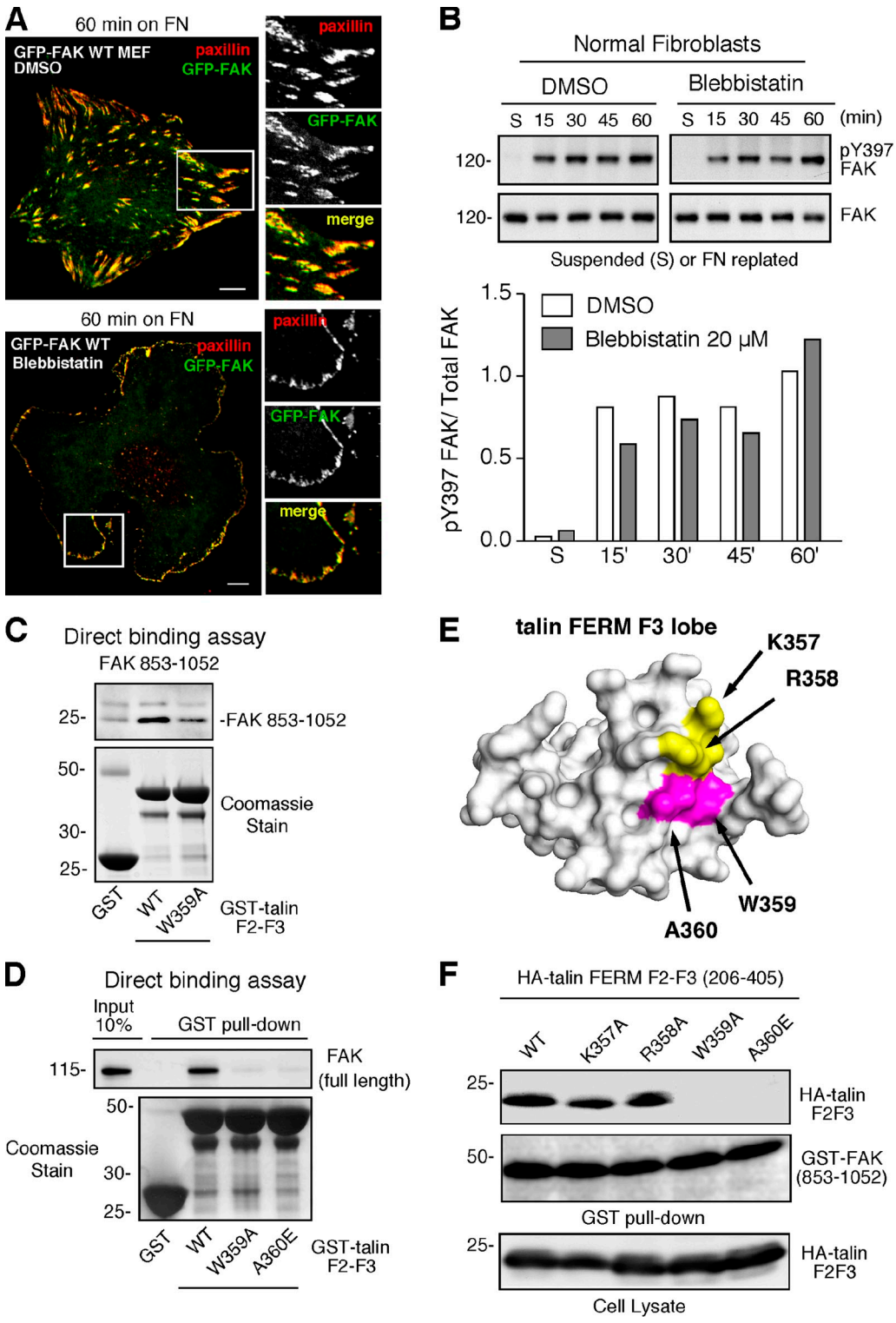


Figure S2. **Tension-independent FAK localization and activation at nascent adhesions.** Direct binding between FAK and talin. (A) FAK$^{-/-}$ MEFs stably re-expressing GFP-FAK WT were serum starved, suspended for 30 min in the presence or absence of 20 µM blebbistatin, plated onto FN-coated coverslips for 60 min, and costained for paxillin (red) or GFP-FAK (green). Merged images show colocalization (yellow). Inset, enlarged area of peripheral adhesion staining. Bar, 10 µm. (B) MEFs were suspended (S) for 30 min or plated on FN for the indicated times in the presence or absence of 20 µM blebbistatin. FAK was immunoprecipitated and evaluated for pY397 or total FAK levels by immunoblotting. Below is a graph that shows densitometry analyses of pY397 to total FAK levels in control (DMSO) or blebbistatin-treated cells. The data shown are from a single representative experiment out of two replicates. (C) GST, GST-talin FERM F2-F3 WT, or GST-talin FERM F2-F3 W359A (5 µg) attached to beads were incubated with purified FAK 852–1052 (350 ng, 0.1 µM), and the amount of direct FAK binding was visualized by anti-FAK immunoblotting. GST or GST-talin FERM F2-F3 were visualized by Coomassie staining. (D) Talin FERM mutations block binding to full-length FAK. FAK was in vitro translated in the presence of biotin-lysine and incubated with beads prebound to GST, GST-talin F2-F3, or GST-talin F2-F3 containing the indicated mutations. Binding was evaluated by streptavidin immunoblotting with 10% of FAK input as a positive control. GST pull-down shows GST or GST-talin FERM F2-F3 levels by Coomassie staining. (E) Crystal structure of the F3 lobe of the talin FERM domain (Wegener et al., 2007). Highlighted are residues K357 and R358 (yellow) important for talin FERM binding to PIPKγ or W359 and A360 (red) important for talin FERM binding to PIPKγ and β-integrins (Barsukov et al., 2003; García-Alvarez et al., 2003; Bouaouina et al., 2008). (F) GST-FAK 853–1,052 binding to talin FERM F2-F3 in 293T cell lysates. The indicated constructs were cotransfected in 293T cells, and GST pull-downs were evaluated by HA tag or GST blotting for talin FERM and GST-FAK, respectively. Blotting of whole cell lysates confirmed equal talin FERM F2-F3 domain expression. Molecular masses are indicated next to the gel blots in kilodaltons.

Published January 23, 2012

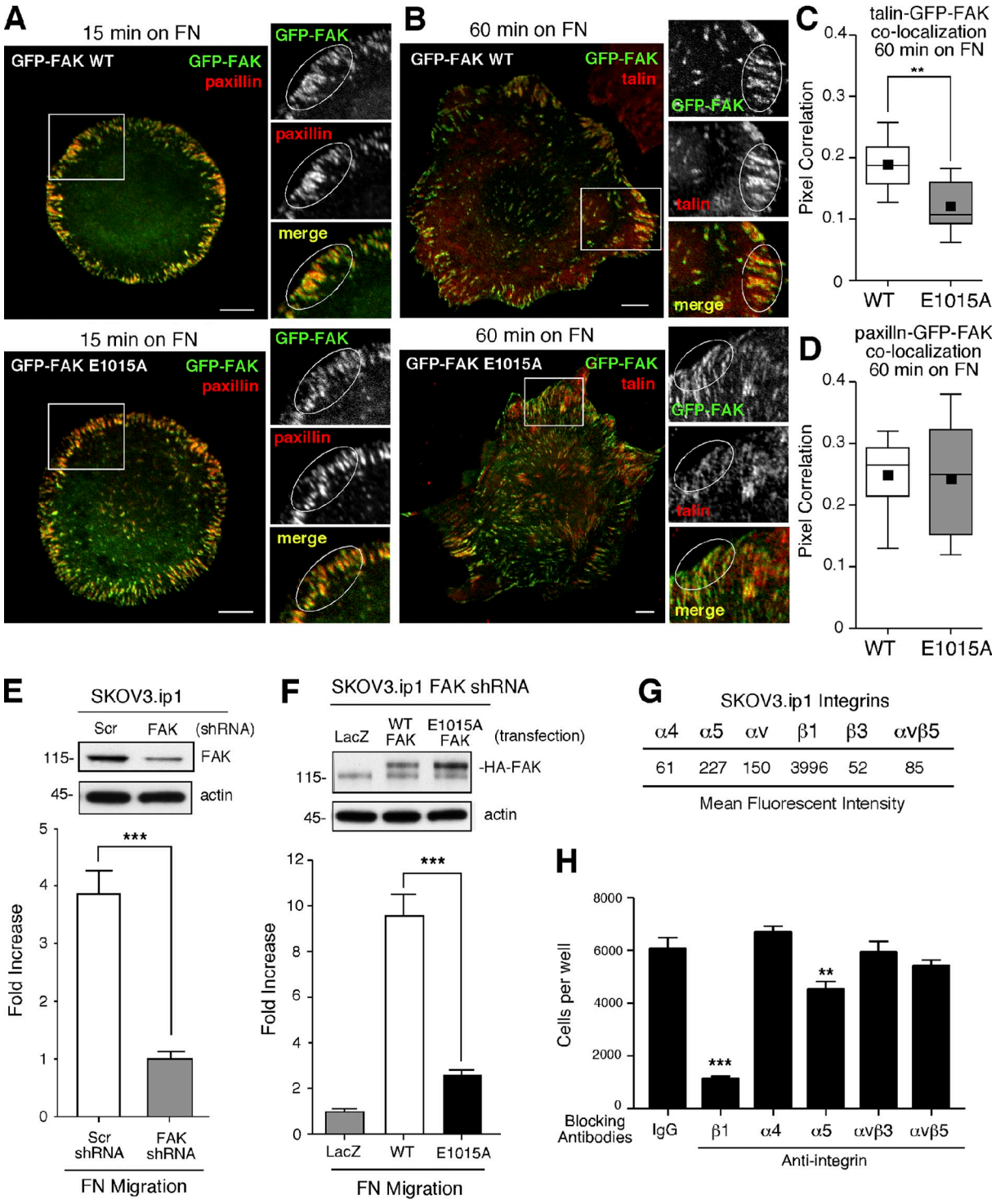


Figure S3. **FAK E1015A localizes to nascent adhesions but does not promote β1 integrin–mediated cell motility.** (A–D) FAK$^{-/-}$ MEFs stably expressing GFP-FAK WT or GFP-FAK E1015A were plated onto FN-coated coverslips for 15 min (A) or 60 min (B), then stained for paxillin (red) and imaged for GFP-FAK (green) fluorescence (A). At 60 min on FN, cells were analyzed for GFP-FAK (green) and talin (red) colocalization (B). The merged image shows colocalization (yellow). Inset, enlarged area of peripheral adhesion staining (circled). Bar, 10 µm. (C and D) The degree of association exhibited by patterns of GFP-FAK and talin (C) or GFP-FAK and paxillin (D) staining was measured on a pixel-by-pixel basis within all adhesions in at least 10 cells per experimental group encompassing at least three independent experiments. Box and whisker plots show the distribution of the data: black square, mean; bottom line, 25th percentile; middle line, median; top line, 75th percentile; whiskers, fifth and 95th percentiles (**, $P < 0.01$). (E) Ovarian SKOV3.ip1 carcinoma cells expressing lentiviral FAK shRNA (or scrambled as control; Scr) were immunoblotted (top) for FAK and actin. (E, bottom) The indicated cells were evaluated for FN-stimulated (10 µg/ml) cell migration (3 h). Data represent the mean ± SEM of three independent experiments (error bars) where FAK shRNA-expressing cell motility was normalized to 1. Significance was determined using an unpaired two-tailed Student's *t* test (***, $P < 0.001$). (F) SKOV3.ip1 FAK shRNA-expressing cells were transiently cotransfected with pCDNA3.1-lacZ and either control vector, HA-tagged FAK-WT, or HA-tagged FAK-E1015A and were immunoblotted (top) for FAK and actin. (F, bottom) The indicated cells were evaluated for FN-stimulated (10 µg/ml) cell migration (3 h). Migratory cells were identified by β-gal staining and counted. Data represent the mean ± SEM of three independent experiments (error bars) where LacZ-transfected cell motility was normalized to 1. Significance was determined using a one-way ANOVA followed by a Tukey multiple comparison test (***, $P < 0.001$). (G) Flow cytometry was used to determine integrin α4, α5, αv, β1, β3, and αvβ5 surface expression, and values represent mean fluorescent intensity using mouse IgG as a control. (H) SKOV3.ip1 cell adhesion to FN-coated (2 µg/ml) dishes was evaluated in the presence of the indicated blocking antibodies to integrins or control IgG. After 15 min, adherent cells were enumerated, and the data represent the mean ± SEM from two independent experiments (error bars). Significance was determined using a one-way ANOVA followed by a Dunnett's multiple comparison test and compared with mouse IgG control group (**, $P < 0.01$; ***, $P < 0.001$).

Published January 23, 2012

Table S1. **Primers used for PCR cloning, PCR mutagenesis, and FAK shRNA**

| Primer | Sequence | Note |
|---|---|---|
| FAK_853_BamHI-5′ | 5′-AAAggatccGGTCCGACTGGAAACCAACAC-3′ | FAK 853–1,052, 853–1,042, 853–1,010, 853–975, and 853–946 in pEBG |
| FAK_881_BamHI-5′ | 5′-AAAggatccCCTGGCCACCTAAGCAACCTG -3′ | FAK 881–1,052 in pEBG |
| FAK_913_BamHI-5′ | 5′-AAAggatccCCCACTGCCAACCTTGACCGG -3′ | FAK 913–1,052 in pEBG |
| FAK_947_BamHI-5′ | 5′-AAAggatccCCAGAAGAGTACGTCCCTATG-3′ | FAK 947–1,052 and 947–1,042 pEBG |
| FAK_976_BamHI-5′ | 5′-AAAggatccCCAGCCAGCACTCATCGAGAG-3′ | FAK 976–1,010 and 976–1,042 in pEBG |
| FAK_1011_BamHI-5′ | 5′-AAAggatccAGCCTGCAGCAGGAGTATTAAG-3′ | FAK 1,011–1,042 in pEBG |
| FAK_S1011A_ BamHI-5′ | 5′-AAAggatcc**GC**CCTGCAGCAGGAGTATAAG-3′ | Site mutagenesis of FAK 1,011–1,042 in pEBG |
| FAK_L1012A_BamHI-5′ | 5′-AAAggatccAGC**GC**GCAGCAGGAGTATAAG-3′ | Site mutagenesis of FAK 1,011–1,042 in pEBG |
| FAK_Q1013A_BamHI-5′ | 5′-AAAggatccAGCCTG**GC**GCAGGAGTATAAG-3′ | Site mutagenesis of FAK 1,011–1,042 in pEBG |
| FAK_Q1014A_BamHI-5′ | 5′-AAAggatccAGCCTGCAG**GC**GGAGTATAAG-3′ | Site mutagenesis of FAK 1,011–1,042 in pEBG |
| FAK_E1015A_BamHI-5′ | 5′-AAAggatccAGCCTGCAGCAGG**C**GTATAAG-3′ | Site mutagenesis of FAK 1,011–1,042 in pEBG |
| FAK_Y1016A_BamHI-5′ | 5′-AAAggatccAGCCTGCAGCAGGAG**GC**TAAG-3′ | Site mutagenesis of FAK 1,011–1,042 in pEBG |
| FAK_1052_ClaI-3′ | 5′-AAAatcgatTCAGTGTGGCCGTGTCTGCCC-3′ | FAK 853–1052, 881–1,052, 913–1,052, and 947–1,052 in pEBG |
| FAK_1042_ClaI-3′ | 5′-AAAatcgatTCATCTTGCTTGATCAATAAC-3′ | FAK 853–1,042, 1,011–1,042, 947–1,042, and 976–1,042 in pEBG |
| FAK_1010_ClaI-3′ | 5′-AAAatcgatTCAGGTCATGACGTACTGCTG-3′ | FAK 853–1,010 and 976–1,010 in pEBG |
| FAK_976_ClaI-3′ | 5′-AAAatcgatTCAAAGAGCAGGAATGGTCTC-3′ | FAK 853–976 in pEBG |
| FAK_946_ClaI-3′ | 5′-AAAatcgatTCAAGGAGCTGGCTGGATTTT-3′ | FAK 853–946 in pEBG |
| FAK_E1015A-5′ | 5′-ACCAGCCTGCAGCAGG**C**GTATAAGAAGCAGATG-3′ | Full length FAK site mutagenesis in pEGFP-C1 and PCDNA 3.1 |
| FAK_E1015A-3′ | 5′-CATCTGCTTCTTATAC**G**CCTGCTGCAGGCTGGT-3′ | Full length FAK site mutagenesis pEGFP-C1 and PCDNA 3.1 |
| Talin F2-F3-BamHI-5′ | 5′ TTTTTTggatccTCCCGAGACCCTGTACAG-3′ | PCR for cloning talin F2-F3 in pGEX-4T1 |
| Talin F2-F3-XhoI-3′ | 5′-TTTTTTctcgagTCACTTACTAGCTTTTTTTCTTC-3′ | PCR for cloning talin F2-F3 in pGEX-4T1 |
| Scrambled shRNA sense | 5′-tGTCTCCGAACGTGTCACGTTtcaagagAACGTGACACGTTCGGAGAC*ttttt*c-3′ | Scrambled shRNA cloning in pLentilox 3.7 |
| Scrambled shRNA antisense | 5′-tcgagaaaaaagtcTCCGAACGTGTCACGTTctcttgaAACGTGACACGTTCGGAGACa-3′ | Scrambled shRNA cloning in pLentilox 3.7 |
| FAK shRNA sens | 5′-tGAACCTCGCAGTCATTTATTtcaagagAATAAATGACTGCGAGGTTC*ttttt*c-3′ | FAK shRNA cloning in pLentilox 3.7 |
| FAK shRNA antisense | 5′-tctagaaaaaagaaCCTCGCAGTCATTTATTctcttgaAATAAATGACTGCGAGGTTCa-3′ | FAK shRNA cloning in pLentilox 3.7 |

Lowercase characters represent restriction enzyme sites. Mutated nucleotides are shown in bold text. 5′ represents forward and 3′ reverse for primers. Italicized characters are accessory components of shRNA. Underlined characters represent stop codons.

## References


Barsukov, I.L., A. Prescot, N. Bate, B. Patel, D.N. Floyd, N. Bhanji, C.R. Bagshaw, K. Letinic, G. Di Paolo, P. De Camilli, et al. 2003. Phosphatidylinositol phosphate kinase type 1gamma and β1-integrin cytoplasmic domain bind to the same region in the talin FERM domain. *J. Biol. Chem.* 278:31202–31209. http://dx.doi.org/10.1074/jbc.M303850200

Bouaouina, M., Y. Lad, and D.A. Calderwood. 2008. The N-terminal domains of talin cooperate with the phosphotyrosine binding-like domain to activate beta1 and beta3 integrins. *J. Biol. Chem.* 283:6118–6125. http://dx.doi.org/10.1074/jbc.M709527200

García-Alvarez, B., J.M. de Pereda, D.A. Calderwood, T.S. Ulmer, D. Critchley, I.D. Campbell, M.H. Ginsberg, and R.C. Liddington. 2003. Structural determinants of integrin recognition by talin. *Mol. Cell.* 11:49–58. http://dx.doi.org/10.1016/S1097-2765(02)00823-7

Wegener, K.L., A.W. Partridge, J. Han, A.R. Pickford, R.C. Liddington, M.H. Ginsberg, and I.D. Campbell. 2007. Structural basis of integrin activation by talin. *Cell.* 128:171–182. http://dx.doi.org/10.1016/j.cell.2006.10.048